Original Research

Synthesis and analysis of small molecules to restrain the function of tissue factor within tumour cells

Oluremi I Adeniran[1], Mohammad A Mohammad[2], Sophie Featherby[2], Anthony Maraveyas[3], Andrew N Boa[1] , Camille Ettelaie[2],*

[1]Department of Chemistry, University of Hull, HU6 7RX Hull, UK, [2]Biomedical Section, University of Hull, HU6 7RX Hull, UK, [3]Division of Cancer-Hull York Medical School, University of Hull, HU6 7RX Hull, UK

TABLE OF CONTENTS

1. Abstract

Introduction: The restriction of prolyl-protein cis/trans isomerase 1 (Pin1) activity has been shown to prevent the release of tissue factor (TF) leading to the accumulation of the latter protein within the cell. This study tested the ability of novel small molecules to inhibit Pin1, suppress TF activity and release, and induce cellular apoptosis. **Methods**: Four compounds were designed and synthesised based on modification of 5-(p-methoxyphenyl)-2-methylfuran-3-carbonyl amide and the outcome on MDA-MB-231 and primary cells examined. These compounds contained 3-(2-naphthyl)-$_D$-alanine (**4a**), $_D$-tryptophan (**4b**), $_D$-phenylalanine (**4c**), and $_D$-tyrosine (**4d**) at the amino-termini. **Results**: Treatment of cells with compound **4b** and **4d** reduced the cell-surface TF activity after 60 min on MDA-MB-231 cells. Incubation with compound **4d** also reduced TF antigen on the

cell surface and its incorporation into microvesicles, while compounds **4a** and **4b** significantly increased TF release. None of the four compounds significantly altered the total amount of TF antigen or TF mRNA expression. Compound **4b** and **4d** also suppressed the binding of Pin1 to TF-cytoplasmic domain peptide. However, compound **4d** reduced while compound **4b** increased the Pin1 isomerase activity. Finally, treatment with compound **4b** and **4d** reduced the cell numbers, increased nuclear localisation of p53, Bax protein and bax mRNA expression and induced cellular apoptosis in MDA-MB-231 but not primary endothelial cells. **Conclusions**: In conclusion, we have identified small molecules to regulate the function of TF within cells. Two of these compounds may prove to be beneficial in moderating TF function specifically and restrain TF-mediated tumour growth without detrimental outcomes on normal vascular cells.

2. Introduction

Regulation of tissue factor (TF) activity and its release as microvesicles is imperative to ensure adequate coagulation during injury, without endangering the precipitation of thrombosis. Consequently, the procoagulant activity of TF is precisely regulated through various mechanisms that influence the TF protein [1–3]. Recently it was demonstrated that the activity and release of TF can be controlled through the action of peptidyl-prolyl *trans/cis* isomerase 1 (Pin1) [4, 5]. Pin1 is a regulator of post-phosphorylation processes and binds to the phosphoserine-proline (termed an MPM-2) motif [6–15]. Normally *trans↔ cis* isomerisation of the peptide bonds occurs at a slow rate and the energy barrier for isomerisation is relatively high. However, the rotation of the peptide bond between the phosphoserine and the proline may be facilitated by enzymes including Pin1. The phosphorylation of serine 258 within the cytoplasmic domain of TF produces such a phosphoserine-proline motif which is a target for Pin1 [16–18]. Since the *trans* configuration is the more prevalent of the two isomers, Pin1 preferentially catalyses the formation of the *cis* isomer. The *cis* isomer is often not accessible to enzymes which bring about subsequent modifications including ubiquitination [10, 12] and de-phosphorylation [19]. The action of Pin1 on the cytoplasmic domain of TF prevents the de-phosphorylation of serine 253 within the cytoplasmic domain of TF. This extends the release of TF within microvesicles by preventing TF ubiquitination [4, 20]. Pin1 has also been reported to prolong the activity of TF and also induce the *de novo* expression of TF mRNA [5]. In addition to the procoagulant activity, TF is known to promote signalling mechanisms that can give rise to cell proliferation [21–23] or alternatively cell apoptosis [24–26]. The inability of cells to dispose of excess TF efficiently appears to contribute to the induction of cell apoptosis, mediated via p53 nuclear localisation and the expression of Bax protein [24, 27, 28]. More-

over, although it has been established that Pin1 is capable of influencing p53 function directly [13, 29–32], there also appears to be an independent regulation mediated through TF.

Previously, we examined the modifications and release of TF in the presence of the non-selective Pin1 inhibitor, juglone. Recently, a number of small molecule Pin1 inhibitors have been designed and tested for their effectiveness as a means of regulating the cell function and particularly, in controlling the proliferation of cancer cells [33, 34]. Using a combination of NMR based fragment screening, co-crystallisation studies and structure-guided design, Potter *et al.* [35, 36] reported the structure of several potent Pin1 inhibitors. Initial studies using NMR screening identified the substance as 5-methylindole 2-carboxylic acid (**1**) (Fig. 1A) and from subsequent fragment co-crystallisation studies, 5-methylbenzimidazole 2-carboxylic acid (**2**) was identified as a more potent building block. Finally, this compound was redesigned into the complex derivative **3** which had a Pin1 IC_{50} of 0.13 μM. However, this proved ultimately to be of limited potential since it lacked any cellular potency. To reduce the polar surface area of the molecule, the benzimidazole was replaced with the 2-naphthyl group, using the commercially available ($_D$)-2-naphthylalanine, to provide the derivative 2'-methyl-5'-(*p*-methoxyphenyl)-3'-furoyl-3-(2-naphthyl)-$_D$-alanine (**4a**). This compound proved to be less potent than 2 against Pin1 (IC_{50} 2.6 μM) but was active in intact cells. In this study, we based a set of small molecules on 5-(*p*-methoxyphenyl)-2-methylfuran-3-carbonyl amide and modified the 'head groups' to modulate the inhibitor-protein interactions. We synthesised and tested four compounds that differed in the amino termini to contain $_D$-tryptophan (**4b**), $_D$-phenylalanine (**4c**), and $_D$-tyrosine (**4d**), as well as the previously reported 3-(2-naphthyl)-$_D$-alanine (**4a**). We then examined the effectiveness of these compounds to alter the activity, expression and release of TF, as well as the potential to block Pin1 activity and its interaction with the cytoplasmic peptide of TF. Finally, the influence of the compounds on the promotion of cell apoptosis, p53 nuclear localisation and Bax/bax expression was assessed.

3. Material and methods

3.1 Synthesis and analysis of potential Pin1 inhibitor compounds

Following the identification of **4a** as a functional compound, derivatives in which the ($_D$)-naphthylalanine moiety was replaced with other aromatic ($_D$)-amino acids (tryptophan, phenylalanine and tyrosine) were envisaged. As a result, a set of four compounds (Fig. 1B) were synthesized (see Supplementary material) based on 5-(*p*-methoxyphenyl)-2-methylfuran-3-carbonyl amide, with a view to examining their structure-activity relationship.

A)

B)

compound	4a	4b	4c	4d
R		—NH		—OH
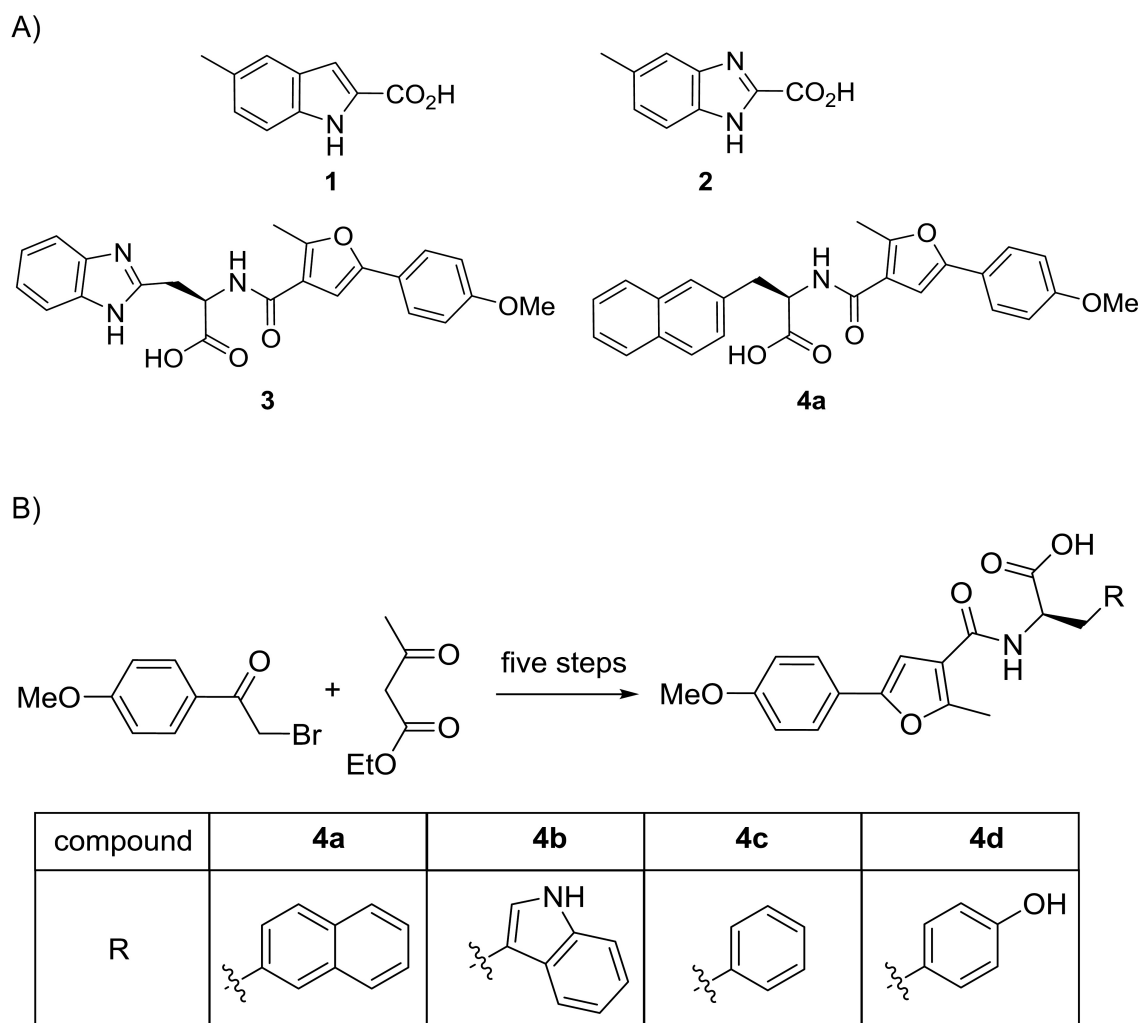
Fig. 1. Structure (A) and synthesis (B) of potential Pin1 inhibitors. Synthesis of the compounds is detailed in the supplementary material. The procedure for the preparation of derivatives was modified substituting the ($_D$)-naphthylalanine moiety with other aromatic ($_D$)-amino acids; tyrosine, tryptophan and phenylalanine. As a result, a set of four compounds were prepared based on 5-(*p*-methoxyphenyl)-2-methylfuran-3-carbonyl amide and synthesised to include (**4a**) 3-(2-naphthyl)-$_D$-alanine, (**4b**) $_D$-tryptophan, (**4c**) $_D$-phenylalanine and (**4d**) $_D$-tyrosine, as the head-groups.

Prior to testing of the biological potential of the synthesised compounds in cells, the structure and purity of the compounds were confirmed. Purification was achieved via column chromatography using Merck 200-300 mesh silica gel, and for thin layer chromatography (TLC) Merck 60 mesh size pre-coated aluminium plates were used. Visualization of TLC bands was achieved using a UV lamp at 254 nm. NMR spectra were obtained using a Jeol JNM ECP400 spectrometer (Welwyn Garden City, UK). ES-MS data were collected on HCT ultra ETD II mass spectrometer (KRSS Europe BV, Veenendaal, Netherlands) and melting points were recorded using a Fisher-Johns apparatus in open capillary tubes. CHN combustion elemental microanalyses were performed using a Carlo-Erba EA1108 CHN Analyzer (Fisons, Loughborough, UK).

3.2 Cell culture, determination of cell numbers and apoptosis assays

MDA-MB-231 breast cancer cell lines (ATCC, Teddington, UK) were cultured in DMEM containing 10% (v/v) FCS. Human dermal blood microvascular endothelial cells (HDBEC; PromoCell, Heidelberg, Germany), devoid of endogenous TF were cultured in MV media containing 5% (v/v) foetal calf serum (FCS) and growth supplements (PromoCell). Cells (5×10^4) were seeded out into 48-well plates and treated with the set of inhibitor compounds (100 μM) or the DMSO vehicle for 24 h. Cell numbers were determined by staining with crystal violet as previously described [37, 38] and calculated from a standard curve. In addition, cellular apoptosis was quantified using the TiterTACS™ Colorimetric Apoptosis Detection Kit (AMS Biotechnology, Abingdon, UK) according to the manufacturer's instructions [26, 39].

3.3 Pin1 activity assay

We previously showed that active Pin1 was capable of binding a synthetic phosphorylated substrate peptide corresponding to the last 18 amino acids of the cytoplasmic domain of TF [4]. A biotinylated form of the phosphorylated peptide (biotin-RKAGVGQSWKENpSPLNVS) was synthesised (Biomatik, Ontario, Canada) and used here as a means of detecting Pin1 binding activity in vitro. An additional scrambled peptide (biotin-SWGNVSKLSAPRQGVNKE) was also included alongside as control. The measurements were carried out as outlined previously [4]. Briefly, the peptides (5 μM final concentration) were diluted to 100 μL with PBS and distributed (50 μL per well) in a NeutrAvidin-coated 96-well plate (Thermo Scientific, Warrington, UK) and incubated for 2 h at room temperature to allow binding. The wells were washed four times, each time with 300 μL of PBST. Sets of wells were supplemented with a range of synthetic inhibitor compounds (0–100 μM) or DMSO vehicle. HRP-conjugated recombinant Pin1 protein was then diluted 1:500 (v/v) in PBST, added to the wells (100 μL) and incubated for 1 h at room temperature. The wells were then washed a further four times and developed with TMB One Solution (100 μL; Promega Corporation, Southampton, UK). Once the colour was developed the reactions were stopped by the addition of 2M sulphuric acid (50 μL) and absorptions measured at 450 nm using a plate-reader. The concentrations of Pin1 were determined from a standard curve made using HRP-conjugated recombinant Pin1 protein.

The isomerase activity of Pin1 was also examined using a previously described procedure [4, 40]. Pin1 was incubated with penta-peptides, Succ-ENSPL-pNitroanilide and Succ-ENpSPL-pNitroanilide and alterations in spectroscopic absorption of the solution analysed. Briefly, samples (100 μL) of the substrate peptides (0.5 μM) were in turn placed in a microcuvette. Recombinant HRP-conjugated Pin1 (10 nM final concentration) was then pre-incubated (5 min) with the inhibitors and then added to the cuvettes. The change in absorption at 315 nm over time was then immediately monitored.

3.4 Cell-based factor Xa-generation assay

Cell surface TF-fVIIa activity was measured by modification of previously described procedures [4]. MDA-MB-231 cells (5 $\times$ 10^4) were incubated with the compound inhibitors (100 μM) diluted in the reaction buffer (100 μL; HEPES-buffered saline (HBS) pH 7.4, containing 1% (w/v) bovine serum albumin (BSA) and 5 mM CaCl$_2$) for 60 min. The cells were washed and incubated with fVIIa (20 nM; Enzyme Research Labs, Swansea, UK) in the reaction buffer for an additional 10 min and then supplemented with fX (100 nM), together with fXa substrate (0.2 mM; Hyphen) diluted in the same buffer (100 μL). The samples were incubated for 60 min to develop the colour. Aliquots (150 μL) were then transferred to a 96-well plate containing 2% (v/v) acetic acid (50 μL) and the absorptions measured immediately at 405 nm. The amount of fXa generated was determined using a standard curve prepared using fXa (Enzyme Research Labs, Swansea, UK). To confirm the cell surface TF activity, cells were pre-incubated with the inhibitory anti-TF antibody HTF1 (40 μg/mL; eBioscience/Thermo Scientific, Warrington, UK) prior to the addition of fVIIa.

3.5 Analysis of cell surface and microvesicles-associated TF antigens

MDA-MB-231 cells (5 $\times$ 10^4) were seeded out into 48-well plates and incubated with the inhibitor compounds as above (100 μM) for 18 h. The cells were then washed with PBS and fixed with 3% (v/v) formaldehyde. The cells were incubated with an HRP-conjugated sheep anti-human TF antibody (100 μL, Enzyme Research Labs., Swansea, UK) diluted 1:1000 (v/v) in PBS for 1 h. The cells were then washed four times with PBS and developed using TMB One Solution substrate Solution (100 μL). Once the colour was developed the reactions were stopped by the addition of 2M sulphuric acid (50 μL) and absorptions measured at 450 nm using a plate-reader. Microvesicle-associated TF antigen was measured using the Quantikine TF-ELISA kit (R&D Systems, Abingdon, UK) according to the manufacturer's instructions.

3.6 Western blot analysis of p53 and Bax proteins

Cells were incubated overnight with the compound inhibitors as above. The cells were then lysed in Laemmli's buffer containing a protease inhibitor cocktail (Sigma Chemical Company, Poole, UK) and equal amounts were separated by 12% (w/v) SDS-PAGE. The protein bands were transferred onto nitrocellulose membranes and blocked with TBST (10 mM Tris-HCl pH 7.4, 150 mM NaCl, 0.05% Tween-20). The membranes were then probed with a polyclonal rabbit anti-human p53 antibody (Cell Signalling Technologies/New England Biolabs, Hitchin, UK) or a mouse monoclonal anti-human Bax antibody (202; Santa Cruz Biotechnology, Heidelberg, Germany), diluted 1:3000 (v/v) in TBST. The membranes were then washed with TBST and probed with a goat anti-rabbit or goat anti-mouse alkaline phosphatase-conjugated antibody (Santa Cruz Biotechnology, Heidelberg, Germany) diluted 1:1000 (v/v) and incubated for 90 min. The bands were then visualised using the Western Blue stabilised alkaline phosphatase-substrate (Promega Corporation Ltd, Southampton, UK) and recorded. All quantifications were normalised against GAPDH which was detected using a polyclonal goat anti-GAPDH antibody diluted 1:5000 (v/v) and then detected using an alkaline phosphatase-conjugated donkey anti-goat-IgG antibody (Santa Cruz Biotechnology, Heidelberg, Germany) diluted 1:2000 (v/v).

3.7 Quantification of TF and bax mRNA expression by quantitative real-time RT-PCR

Total RNA was isolated using the TRI-reagent system (Sigma Chemical Company, Poole, UK) from 2×10^5 cells and 100 ng of total RNA was used for each reaction. The relative amounts of TF or bax mRNA were determined using QuantiTect primer sets to detect either TF or bax, in conjunction with β-actin (Qiagen, Manchester, UK). The reaction was carried out at an annealing temperature of 60 °C for 1 min using the GoTaq® 1-Step RT-qPCR System (Promega Corporation Ltd, Southampton, UK) on an iCycler thermal cycler (Bio-Rad, Hemel Hempstead, UK) for 40 cycles. Following amplification, the amounts of mRNA were determined using the $2^{-\Delta\Delta CT}$ method and ratios were calculated [41].

3.8 Analysis of p53 nuclear localisation by fluorescence microscopy

MDA-MB-231 cells (10^3) were seeded out into 35-mm glass-bottom with 10 mm μ-well dishes and incubated for 4 h at 37 °C. The medium was aspirated and replaced with 100 μL of medium supplemented with test reagents (100 μM). Sets of cells were treated with of TNF-α (10 ng/mL) or DMSO and were used as positive and negative controls, respectively. The media were removed after 18 h and the cells were washed twice with PBS (200 μL) and fixed using 4% (v/v) paraformaldehyde. After three further washes with PBS, the cells were permeabilised with 0.2% (v/v) Triton X-100 diluted in PBS and incubated at room temperature for a further 10 min. The samples were then blocked for 1 h with PBS containing 3% (w/v) bovine serum albumin (BSA). The cells were then washed a further three times and probed with a rabbit polyclonal anti-human p53 antibody diluted 1:250 (v/v) in PBS/BSA buffer (100 μL) and incubated overnight, at 4 °C. After a further three washes with PBS, the samples were incubated for 1 h with a Northern Lights-637 donkey anti-rabbit antibody (R&D Systems, Abingdon, UK) diluted 1:100 (v/v) in PBS/BSA buffer (100 μL), in the dark. The cells were then washed another two times with PBS and stained with DAPI (2 μg/mL). Images were acquired using a Zeiss Axio Vert.A1 inverted fluorescence microscope with a $\times 40$ magnification (Carl Zeiss Ltd, Welwyn Garden City, UK). The localisation of p53 within the nuclei were determined using ImageJ program (version 1.48v, LOCI, University of Wisconsin, Madison, WI, USA), in 10 fields of view from each assay and Mander's coefficient determined [42, 43].

3.9 Approximation of binding of compounds to Pin1

The structures of the four compounds were constructed using the Alchemy program (Tripos Associates Inc., St Louis, USA) and then saved in Brookhaven format (PDB). The crystal structures of Pin1 (1PIN) was obtained from Brookhaven format (PDB). The location and efficiency of binding of the compounds to Pin1 was esti-mated using Autodock 4v2.6 [44]. The Autodock graphical interface AutoDockTools 1.5.6 was used, the polar hydrogens were retained and partial charges added to the proteins using the Gasteiger charges. The search space was limited to an area of $20 \times 20 \times 20$ Å, centred around the hydroxyl group of Ser18 in the enzymatic site of Pin1. For each enzyme, $25 \times$ ligand orientations (poses) were examined and ranked according to the scoring-function and inhibition coefficient calculated.

3.10 Statistical analysis

All data represent the calculated mean values from the number of experiments stated in each figure legend $\pm$ the calculated standard error of the mean. Statistical analysis was carried out using the Statistical Package for the Social Sciences v21 (SPSS Inc. Chicago, IL, USA). Significance was determined using one-way ANOVA (analysis of variance) and Tukey's honesty significance test or where appropriate, by paired t-test.

4. Results

4.1 The influence of synthesised inhibitors on Pin1 binding and activity

To determine the inhibitory potential of the synthesised compounds, the ability of the compounds to prevent the substrate binding and isomerase activities of Pin1 was examined. The enzyme used was recombinant HRP-conjugated Pin1 and the target substrate peptide was biotin-RKAGVGQSWKENpSPLNVS (from the cytoplasmic domain of TF) which was described and confirmed previously as a suitable target for Pin1 binding [4]. Inclusion of $_D$-tryptophan (substance **4b**) and $_D$-tyrosine (substance **4d**) head-groups inhibited the Pin1 binding to the substrate peptide with latter being the more efficient inhibitor (Fig. 2A). In contrast, inclusion of $_D$-phenylalanine (substance **4c**) head-group had no significant outcome on Pin1 binding while the addition of 3-(2-naphthyl)-$_D$-alanine (substance **4a**) marginally enhanced Pin1 binding. In addition to the binding assay, the isomerase activity of Pin1 towards a pentapeptide (Succ-ENpSPL-pNitroanilide) was measured spectroscopically in the presence of the synthesised inhibitor substances (Fig. 2B). Analyses of these samples showed a clear decrease in Pin1 isomerase activity with the $_D$-tyrosine derivative (substance **4d**) but not phenylalanine (substance **4c**) derivative. In contrast, an increase in Pin1 isomerase activity was detected on inclusion of 3-(2-naphthyl)-$_D$-alanine (substance **4a**) and $_D$-tryptophan (substance **4b**) head-groups (Fig. 2B).

4.2 The influence of synthesised inhibitors on TF activity, cell-surface and microvesicle-associated TF antigen and TF mRNA expression

To assess the direct influence of the inhibitors on TF activity, MDA-MB-231 cells were pre-incubated for 60

A)

B)
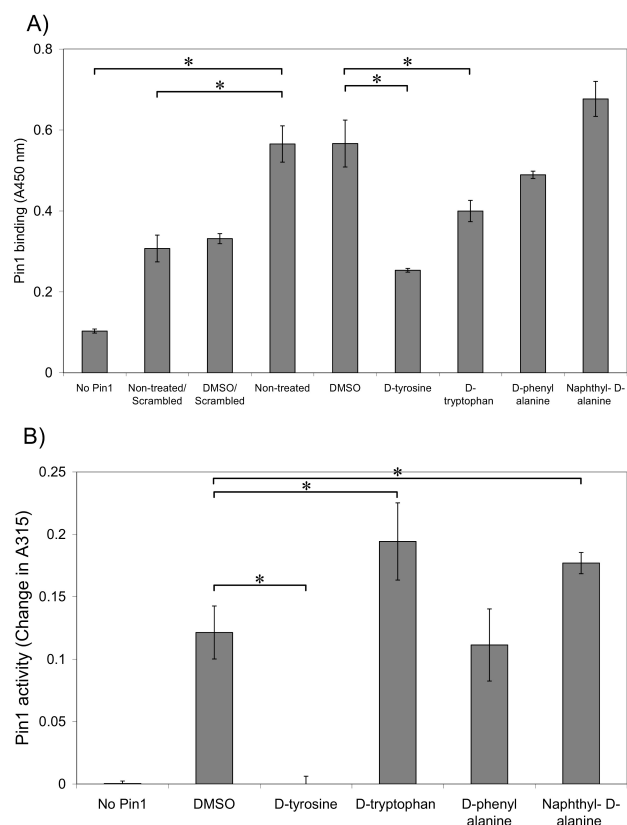
Fig. 2. The influence of the synthesised inhibitors on Pin1 binding and activity. (A) A biotinylated form of the phosphorylated TF peptide (biotin-RKAGVGQSWKENpSPLNVS) was used to capture Pin1 *in vitro* along with a scrambled peptide (biotin-SWGNVSKLSAPRQGVNKE) as control. The peptides (5 μM final concentration) were diluted to 100 μL with PBS and distributed (50 μL per well) in a NeutrAvidin-coated 96-well and incubated for 2 h at room temperature to allow binding. The wells were washed four times, each time with 300 μL of PBST. Sets of wells were supplemented with a range of synthetic inhibitors (0–100 μM) or DMSO vehicle. HRP-conjugated recombinant Pin1 protein was diluted 1:500 (v/v) in PBST, added to the wells (100 μL) and incubated for 1 h at room temperature. The wells were then washed a further four times and developed with TMB One Solution (100 μL). Once the colour was developed the reactions were stopped by the addition of 2M sulphuric acid (50 μL) and absorptions measured at 450 nm using a plate reader. The concentrations of Pin1 were determined from a standard curve made using HRP-conjugated recombinant Pin1 protein (n = 3, * = $p < 0.05$). (B) Pin1 was incubated with penta-peptides, Succ-Glu-Asn-Ser-Pro-Leu-pNitroanilide and Succ-Glu-Asn-phosphoSer-Pro-Leu-pNitroanilide and alterations in spectroscopic absorption of the solution analysed. Briefly, samples (100 μL) of the substrate peptides (0.5 μM) were in turn placed in a microcuvette. Recombinant HRP-conjugated Pin1 (10 nM final concentration) was then pre-incubated (5 min) with the inhibitors and then added to the cuvettes. The change in absorption at 315 nm over time was then immediately monitored (n = 3, * = $p < 0.05$).

min with the synthesised substances and TF activity measured using a chromogenic fXa-generation assay. Inclusion of $_D$-tryptophan (substance **4b**) and $_D$-tyrosine (substance **4d**) head-groups in the compounds inhibited the throm-

bin generation by 38% and 31% respectively (Fig. 3A). In contrast, reductions in TF activity, on inclusion of 3-(2-naphthyl)-$_D$-alanine (substance **4a**) and $_D$-phenylalanine (substance **4c**) derivatives were not significant. Therefore, only the alterations observed on with $_D$-tryptophan (substance **4b**) and $_D$-tyrosine (substance **4d**) derivatives were assumed to be specific.

Incubation of MDA-MB-231 cells with compound **4d**, containing $_D$-tyrosine head-group, resulted in low but significant reduction in cell-surface TF antigen (Fig. 3B) and TF release within microvesicles (Fig. 3C). Moreover, treatment of cells with either substances containing 3-(2-naphthyl)-$_D$-alanine (substance **4a**) or $_D$-tryptophan (substance **4b**) head groups resulted in substantial increases in the release of TF within cell-derived microvesicles (Fig. 3C). Incubation of MDA-MB-231 cells for 6 h with any of the four synthesised compounds, did not result in significant changes in TF mRNA expression (Fig. 3D).

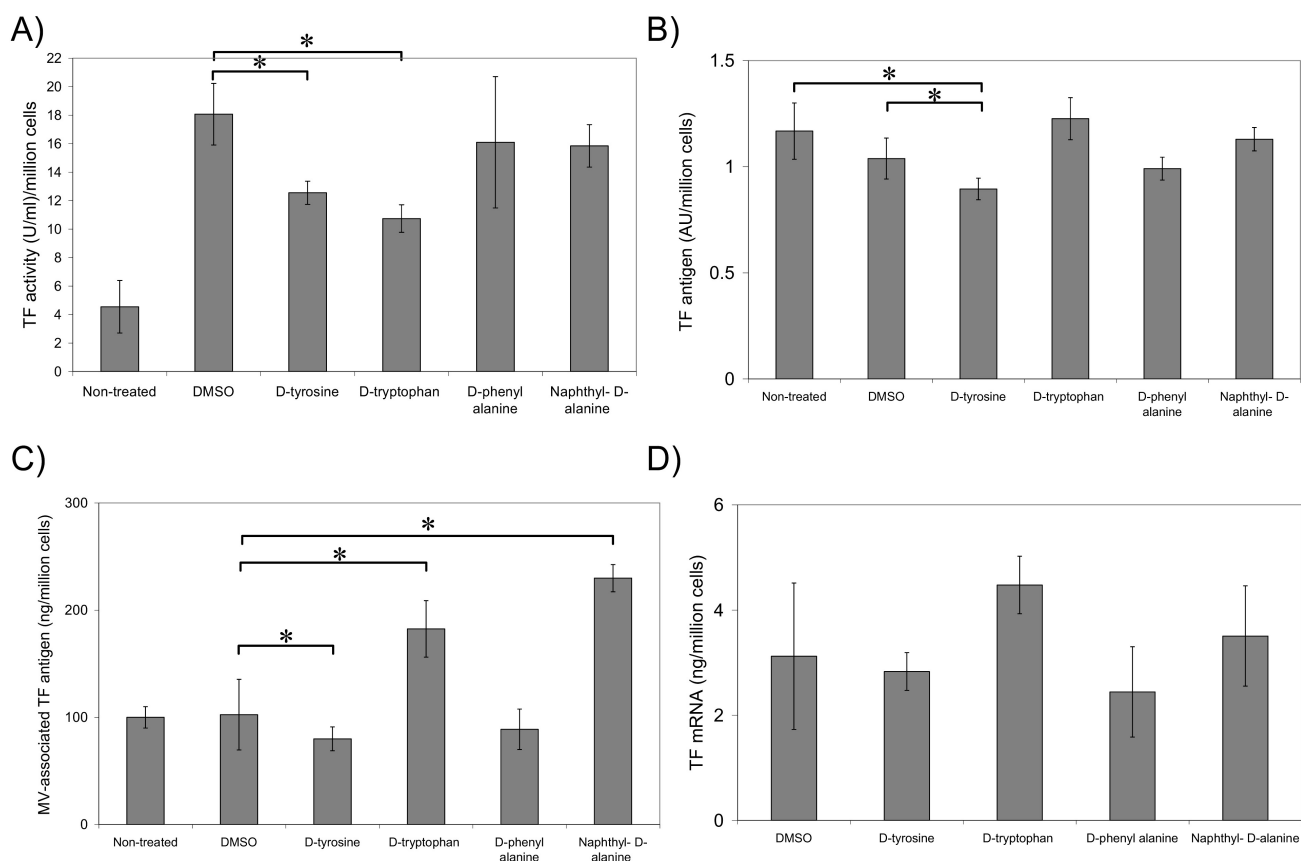### 4.3 The influence of synthesised inhibitors on cellular apoptosis

Incubation of MDA-MB-231 cells with substances containing the 3-(2-naphthyl)-$_D$-alanine (substance **4a**), $_D$-tryptophan (substance **4b**) and $_D$-tyrosine (substance **4d**) head-groups resulted in approximately 22%, 48% and 55% reduction in cell numbers respectively (Fig. 4A) and were associated with significant increases in DNA-fragmentation as measured by the end-labelling TUNEL assay (Fig. 4B). In contrast, the inclusion of $_D$-phenylalanine (substance **4c**) was ineffective. Importantly, incubation of the HDBEC primary cells which are devoid of TF, did not have any detectable influence on cell numbers of the rate of cell apoptosis (Fig. 4C).

4.4 The influence of synthesised inhibitor compounds on Bax expression

To further confirm the mechanism of apoptosis in MDA-MB-231 cells, following treatment with the inhibitors the expression of Bax protein and bax mRNA were measured. $_D$-tyrosine derivative (substance **4d**) and to a lesser extent $_D$-tryptophan derivative (substance **4b**) resulted in increased expression of both Bax protein (Fig. 4D,E) and bax mRNA (Fig. 4F) while the 3-(2-naphthyl)-$_D$-alanine (substance **4a**) and $_D$-phenylalanine (substance **4c**) derivatives were ineffective.

4.5 The influence of synthesised inhibitor compounds on p53 expression and localisation

Finally, since Pin1 can influence cell apoptosis through altering the activity and stability of p53 protein, the influence of synthesised inhibitor substances on the expression and nuclear localisation of p53 was examined. Incubation of MDA-MB-231 cells with $_D$-tyrosine (substance **4d**) containing compound resulted in increased nuclear localisation of p53 compared to the control sample, but was not significant with compounds containing the 3-(2-naphthyl)-

Fig. 3. **The influence of the synthesised inhibitors on TF activity, antigen and mRNA levels.** (A) MDA-MB-231 cells (5×10^4) were incubated with the inhibitors (100 μM) diluted in the reaction buffer (100 μL; HEPES-buffered saline (HBS) pH 7.4, containing 1% (w/v) bovine serum albumin (BSA) and 5 mM CaCl$_2$) for 60 min. The cells were washed and incubated with fVIIa (20 nM) in the reaction buffer for an additional 10 min and then supplemented with fX (100 nM), together with fXa substrate (0.2 mM) diluted in the same buffer (100 μL). The samples were incubated for 60 min to develop the colour. Aliquots (150 μL) were then transferred to a 96-well plate containing 2% (v/v) acetic acid (50 μL) and the absorptions measured immediately at 405 nm. The amount of fXa generated was determined using a standard curve prepared using fXa (n = 5, * = $p < 0.05$). (B) MDA-MB-231 cells (5×10^4) were seeded out into 48-well plates and incubated with the inhibitors as above (100 μM) for 18 h. The cells were then washed with PBS and fixed with 3% (v/v) formaldehyde. The cells were then incubated with an HRP-conjugated sheep anti-human TF antibody (100 μL) diluted 1:1000 (v/v) in PBS for 1 h. The cells were then washed four times with PBS and developed using TMB One Solution substrate Solution (100 μL). Once the colour was developed the reactions were stopped by the addition of 2M sulphuric acid (50 μL) and absorptions measured at 450 nm using a plate reader (n = 5, * = $p < 0.05$). (C) The TF antigen associated with the microvesicles was measured using the Quantikine TF-ELISA kit according to the manufacturers' instructions (n = 3, * = $p < 0.05$). (D) Total RNA was isolated using the TRI-reagent system from 2×10^5 cells and 100 ng of total RNA was used for each reaction. The relative amounts of TF mRNA were determined using QuantiTect primer sets to detect TF in conjunction with β-actin. The reaction was carried out at an annealing temperature of 60 °C for 1 min using the GoTaq® 1-Step RT-qPCR System on an iCycler thermal cycler for 40 cycles (n = 3, * = $p < 0.05$).

$_D$-alanine (substance **4a**), $_D$-tryptophan (substance **4b**) and $_D$-phenylalanine (substance **4c**) head-groups (Fig. 5A,B). Moreover, incubation of the cells with any of the four compounds did not alter the amount of p53 proteins as measured by western blot (Fig. 5C).

4.6 Approximation of binding of compounds to Pin1

The interactions of the four compounds with Pin1 enzyme were examined using the crystal structure of Pin1 (1PIN). The location (Fig. 6) and efficiency of binding of the four compounds to Pin1 was examined using Autodock 4v2.6 software. Estimation of the binding efficiencies indicated a comparable binding energy for all four compounds

(Table 1). However, calculated binding constants indicated a higher affinity for the substances **4a** and **4b** (5.03 μM and 10.97 μM respectively) but lower for substances **4c** and **4d** (28.18 μM and 47.44 μM respectively). A visual inspection of the complexes with Pin1 illustrated similar conformations in three of the docked molecules but indicated interaction with additional residues in the molecule containing the $_D$-tyrosine (substance **4d**) head-group.
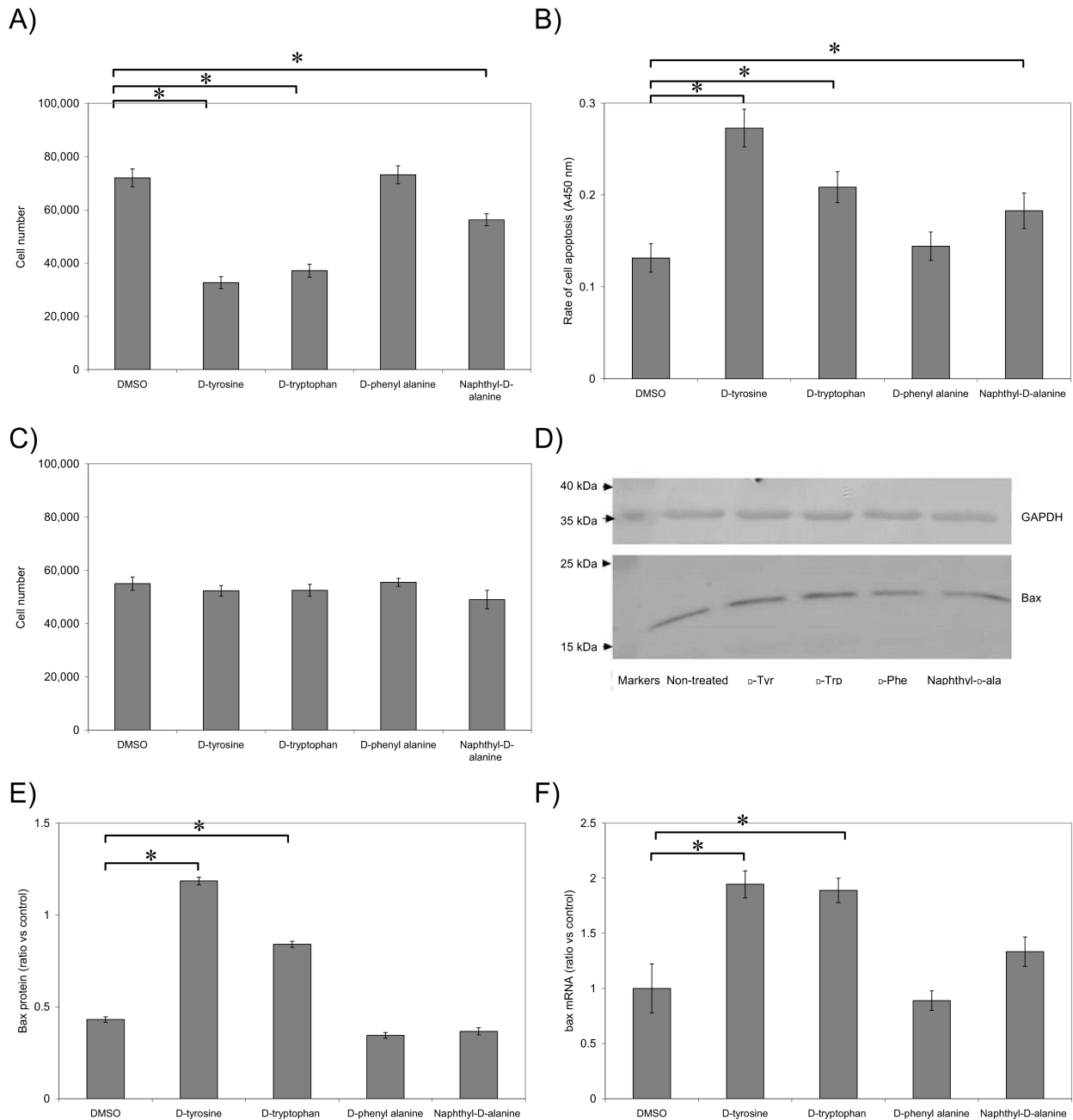
Fig. 4. Examination of the pro-apoptotic potential of the synthesised inhibitors. (A) MDA-MB-231 cells (5×10^4) were seeded out into 48-well plates and treated with the set of inhibitors or the DMSO vehicle. Cell numbers were determined by staining with crystal violet and calculated from a standard curve (n = 5, * = $p < 0.05$). (B) Cellular apoptosis was quantified using the TiterTACS™ Colorimetric Apoptosis Detection Kit according to the manufacturer's instructions (n = 3, * = $p < 0.05$). (C) HDBEC (5×10^4) were seeded out into 48-well plates and treated with the set of inhibitors or the DMSO vehicle. Cell numbers were determined by staining with crystal violet and calculated from a standard curve. (n = 3). (D) Cells (5×10^4) were treated as above and lysed in Laemmeli's buffer containing a protease inhibitor cocktail. Equal amounts were separated by 12% (w/v) SDS-PAGE and the protein bands were transferred onto nitrocellulose membranes and blocked with TBST. The membranes were then probed with a mouse monoclonal anti-human Bax antibody (202), diluted 1:3000 (v/v) in TBST. The membranes were washed with TBST and probed with a goat anti-rabbit or goat anti-mouse alkaline phosphatase-conjugated antibody diluted 1:1000 (v/v) and incubated for 90 min. The bands were then visualised using the Western Blue stabilised alkaline phosphatase-substrate and recorded (Images are representative of 3 separate experiments). (E) All quantifications were normalised against GAPDH which was detected using a polyclonal goat anti-GAPDH antibody diluted 1:5000 (v/v) and then detected using an alkaline phosphatase-conjugated donkey anti-goat-IgG antibody diluted 1:2000 (v/v) (n = 3, * = $p < 0.05$). (F) Total RNA was isolated using the TRI-reagent system from 2×10^5 cells and 100 ng of total RNA was used for each reaction. The relative amounts of bax mRNA was determined using QuantiTect primer sets to detect bax in conjunction with β-actin. The reaction was carried out at an annealing temperature of 60 °C for 1 min using the GoTaq® 1-Step RT-qPCR System on an iCycler thermal cycler for 40 cycles (n = 3, * = $p < 0.05$).
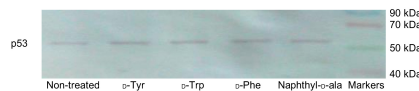
A)
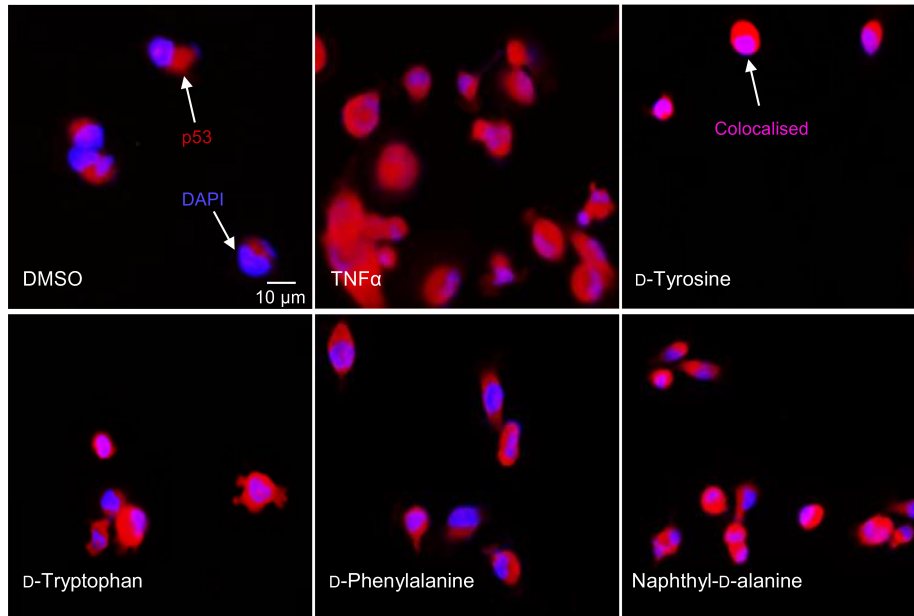
B)
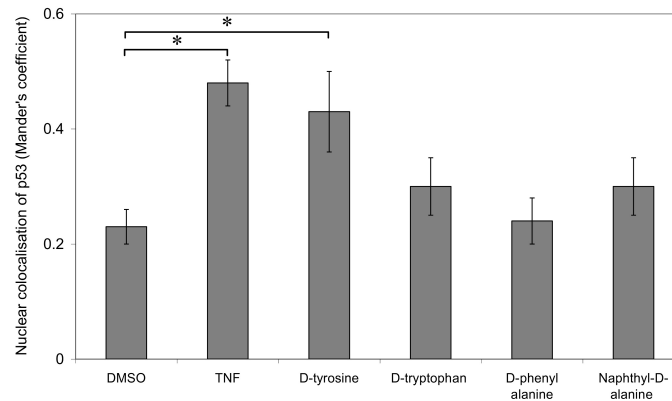
C)

Fig. 5. The influence of the synthesised inhibitors on nuclear localisation of p53. Cells were seeded out into 35-mm glass-bottom with 10 mm μ-well dishes were seeded 10^3 MDA-MB-231 cells and incubated for 4 h at 37 °C in an incubator. The medium was aspirated and replaced with 100 μL of medium supplemented with test agents (100 μM). Sets of cells were treated with of TNF-α (10 ng/mL) or used untreated and used as positive and negative controls, respectively. The media were removed after 18 h and the cells were washed twice with PBS (200 μL) and fixed using 4% (v/v) paraformaldehyde. After three washes with PBS, the cells were permeabilised with 0.2% (v/v) Triton X-100 diluted in PBS and incubated at room temperature for a further 10 min. The samples were then blocked for 1 h with PBS containing 3% (w/v) bovine serum albumin (BSA). The cells were then washed a further three times and probed with a rabbit polyclonal anti-human p53 antibody diluted 1:250 (v/v) in PBS/BSA buffer (100 μL) and incubated overnight, at 4 °C. After a further three washes with PBS, the samples were incubated with a Northern Lights-637 donkey anti-rabbit antibody diluted 1:100 (v/v) PBS/BSA buffer (100 μL), for 1 h in the dark. The cells were washed another two times with PBS and stained with DAPI (2 μg/mL). (A) Images were acquired using a Zeiss Axio Vert.A1 inverted fluorescence microscope with a ×40 magnification (Images are representative of 10 field of view from 3 separate experiments). (B) The localisation of p53 within the nuclei were determined using ImageJ, in 10 fields of view from each assay and Mander's coefficient determined (n = 3, * = $p < 0.05$). (C) Cells (5×10^4) were treated as above and lysed in Laemmeli's buffer containing a protease inhibitor cocktail. Equal amounts were separated by 12% (w/v) SDS-PAGE and the protein bands were transferred onto nitrocellulose membranes and blocked with TBST. The membranes were then probed with a polyclonal rabbit anti-human p53 antibody. The membranes were washed with TBST and probed with a goat anti-rabbit or goat anti-rabbit alkaline phosphatase-conjugated antibody diluted 1:1000 (v/v) and incubated for 90 min. The bands were then visualised using the Western Blue stabilised alkaline phosphatase-substrate and recorded. (Images are representative of 3 separate experiments).
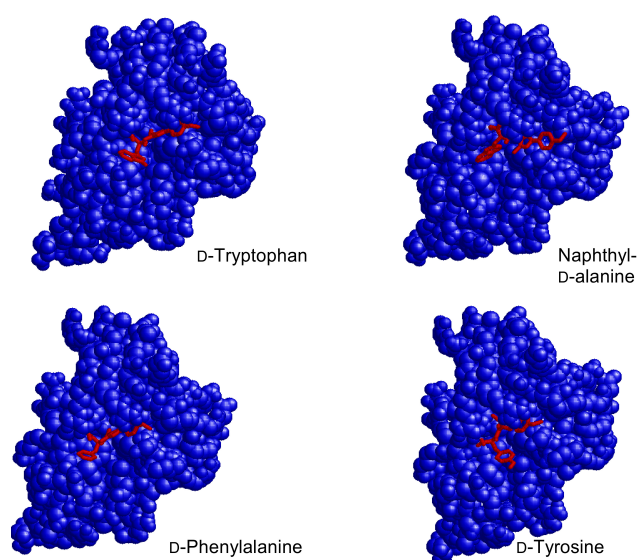
Fig. 6. The influence of the synthesised inhibitors on nuclear localisation of p53. The structure of the four molecules were constructed using the Alchemy program and saved in Brookhaven format (PDB). The crystal structures of Pin1 (1PIN) was obtained from Brookhaven format (PDB). The location and efficiency of binding of the molecules to Pin1 was estimated using the Autodock 4v2.6, the polar hydrogens were retained and partial charges added to the proteins using the Gasteiger charges. The search space was limited to an area of $20 \times 20 \times 20$ Å, centred around the hydroxyl group of Ser18 in the enzymatic site of Pin1.

Table 1. Approximation of binding of molecules to Pin1.

Amino acid incorporated	Binding energy	Apoptosis
D-Tyrosine	–0.20	47.44
D-Tryptophan	–0.22	10.97
D-Phenylalanine	–0.22	28.18
Naphthyl-D-alanine	–0.23	5.03

The structures of the four molecules were constructed using the Alchemy program and saved in Brookhaven format (PDB). The crystal structures of Pin1 (1PIN) was obtained from Brookhaven format (PDB). The location and efficiency of binding of the molecules to Pin1 was estimated using the Autodock 4v2.6. For each enzyme, $25 \times$ ligand orientations (poses) were examined and ranked according to the scoring-function and inhibition coefficient calculated.

5. Discussion

Pin1 is involved in the regulation of a number of cellular processes, particularly those associated with cancer. Pin1 overexpression is often accompanied with the increased function of over 50 anti-apoptotic proteins and repression of over 26 tumour suppressor proteins [34, 45, 46]. Pin1 has also been reported to be a prominent mediator of epithelial-mesenchymal plasticity in cancer cells [47]. As well as cancer cells, Pin1 has also been associated with inflammatory responses during chronic disease such as atherosclerosis and rheumatoid arthritis [48, 49]. The majority of the pro-inflammatory [50] and cancer-related [51, 52] mechanisms stated above have also been firmly associated with TF. The synchroneity between these proteins, and the recent demonstration of the functional interaction of the proteins, suggests an inter-dependence which may be exploited by using small molecules that can concurrently influence the function of both of these other proteins. Such small molecules may include the Pin1 inhibitors as discussed above, as well as the use of certain direct oral anticoagulants (DOAC) which modify the TF-mediated signalling by inhibiting the coagulation enzymes such as factor VIIa, and inducing the activation of p53-mediated cell apoptosis [53, 54]. Moreover, to envision the usage of such small molecules may confer distinct advantages to other strategies that are based on the suppression of gene expression.

Recent studies have indicated differences in the cellular outcomes following suppression of Pin1 expression, compared to strategies that inhibit of Pin1 [55]. Furthermore, variable outcomes have also been reported when using different Pin1-inhibitors [55, 56]. Among the possible mechanisms for such distinct influences, accessibility to different cellular compartments [57] or variability in substrate recognition [58] may explain the underlying differences. The function of Pin1 is closely regulated through a number of post-translational modifications which indicates that Pin1 may be altered [34] in order to comply with the required function when present in different cellular locations or compartments. The ability of Pin1 to regulate the activity of TF and its release from cells suggests a role in the dysregulation of procoagulant activity associated with malignant compared to normal cells. Moreover, the close association of TF with cancer progression and cellular survival indicates that Pin1 may have an indirect homeostatic action as well as the commonly documented functions.

The ability of Pin1 to interact with the phosphorylated form of cytoplasmic domain of TF indicates the participation of membrane proximal/associated Pin1. In this study we envisaged that it may be feasible to prepare a membrane-permeable small-molecule inhibitor to specifically reduce TF activity and release in microvesicles. Consequently, we prepared and evaluated four compounds based on 5-(*p*-methoxyphenyl)-2-methylfuran-3-carbonyl amide, with additional aromatic head-groups to alter the binding capacity to Pin1. Compounds containing D-tryptophan (**4b**) and D-tyrosine (**4d**) 'head groups' were both capable of interfering with the binding of Pin1 to the biotin-RKAGVGQSWKENpSPLNVS peptide. However, while compound **4d** suppressed the Pin1 activity towards the smaller Succ-ENpSPL-pNitroanilide pentapeptide, compound **4b** enhanced this activity. As an insight into the possible differences, the *in silico* analysis of the interaction of the compounds with Pin1 protein, indicated that despite the lower binding affinity, compound **4d** (containing D-tyrosine) was capable of interacting with Pin1

residues which were not engaged by any of the other synthesised compounds (Fig. 6). However, the enhancement of Pin1 activity on incubation with compound **4b**, when tested against the pentapeptide but not the TF-peptide, suggests that the inhibitors function by hindering the interaction of Pin1 with the longer substrate.

The four compounds also exhibited different binding and functional potencies, particularly towards TF activity and function. In agreement with the data published by Kurakula *et al.*, blocking of Pin1-TF interaction in cells, using compounds **4b** or **4d** reduced the fXa generation activity on the surface of cells. Moreover small, but significant decreases in cell surface TF antigen, as well as the incorporation into microvesicles, were observed following the incubation of cells with compound (**4d**) containing $_D$-tyrosine (Fig. 3). However, in agreement with the enhancement of Pin1 isomerase observed with compound **4b** (containing $_D$-tryptophan), higher levels of TF incorporation and release were also observed following the incubation of cells with compound **4b**. Together, these data further suggest that these compounds specifically interfere with the regulation of TF function by Pin1. Therefore, while both compound **4b** and **4d** are capable of preventing the approach of the longer peptides, the presence of acidic tyrosine as the head-group may also hinder the catalytic function of Pin1. Isomerisation of TF on the cell surface by Pin1 is assumed to prolong its presence on the cell surface [5] and allow its incorporation into microvesicles [4]. Therefore, the inhibition of Pin1 would be expected to accelerate the processing and endocytosis of TF into the cells [4, 20, 59]. However, it is possible that compound **4b** may also regulate other molecular components involved in the formation as well as the translocation of proteins into microvesicles. In contrast, our studies did not indicate any alterations in the *de novo* expression of TF following supplementation of cells with either of the compounds as has been previously reported [5]. One explanation for this may arise from the inaccessibility of the nuclear compartment to the inhibitor compounds and suggests that the synthesised compounds are limited to the cytoplasmic/membrane regions [57]. Another possibility may be due to the reported differences in the outcomes which are achieved following Pin1 knockdown or by Pin1 inhibition [55]. Finally, the discrepancy may arise from differences in the duration of incubation prior to mRNA quantification which was 6 h in our studies.

We previously demonstrated that disruptions in the ability of cells to moderate and release TF can result in the activation of pro-apoptotic mechanisms, mediated through src [25] and p38-MAPK [24] activation and leading to the nuclear localisation of p53, upregulation of Bax and induction of cell apoptosis. Consequently, we envisaged that the interruption of the regulation of TF trafficking on the cell surface and reducing the rate of TF processing may initiate these pro-apoptotic mechanisms. Therefore, in addition to the changes in the cell-surface TF antigen and activity, the influence of the synthesised compounds on the homeostatic mechanisms was investigated. In agreement with the above hypothesis, incubation of cells with compound **4d** (containing $_D$-tyrosine) and to a lesser level, with compound **4b** containing $_D$-tryptophan resulted in reduced cell numbers, arising from cell apoptosis as measured by DNA end-labelling and observable within 24 h. Incubation of cells with compound **4a** (containing 3-(2-naphthyl)-$_D$-alanine) also resulted in the reduction in cell numbers. However, none of the pro-apoptotic mediators were altered and together with the non-specific release of TF in microvesicles, these results indicate a non-specific cytotoxic effect by compound **4a**. Interestingly, these outcomes appeared to be specifically mediated through TF since primary endothelial cells were not adversely affected. Furthermore, compound **4d** was able to promote nuclear localisation of p53 which may also arise from the retention of TF, although direct effects of Pin1 on p53 localisation are well documented [30–32]. Finally, in agreement with the above data, compounds **4b** and **4d** were able to induce the expression of bax mRNA and Bax protein which explains the initiation of cell apoptosis.

6. Conclusions

The regulation of the haemostatic and homeostatic functions of TF is a promising direction and a potential therapeutic approach, particularly in cancer. In this study, we aimed to assess the potential for synthetic small compounds, based on previously known structures, to exert a regulatory effect on the procoagulant and signalling properties of TF. Moreover, through targeting TF-mediated cellular pathways, tumour cells but not endothelial cells were selectively eliminated. Of the four synthesised compounds based on 5-(*p*-methoxyphenyl)-2-methylfuran-3-carbonyl amide, the inclusion of $_D$-tyrosine as a head-group produced the most effective, functional and applicable compound and constitutes a basis for further chemical formulations and development for therapeutic exploration.

7. Author contributions

The study was designed by AM, ANB and CE, and the experimental work carried out by OIA, MAM, SF and CE. The data were evaluated by OIA, ANB and CE and the manuscript was prepared by OIA, ANB, AM and CE.

8. Ethics approval and consent to participate

Not applicable.

9. Acknowledgment

Not applicable.

10. Funding

11. Conflict of interest

The authors declare no conflict of interest.

12. References

[1] Grover SP, Mackman N. Tissue Factor: An Essential Mediator of Hemostasis and Trigger of Thrombosis. Arteriosclerosis, Thrombosis, and Vascular Biology. 2018; 38: 709–725.

[2] McVey JH. The role of the tissue factor pathway in haemostasis and beyond. Current Opinion in Hematology. 2016; 23: 453–461.

[3] Chen VM, Hogg PJ. Encryption and decryption of tissue factor. Journal of Thrombosis and Haemostasis. 2013; 11: 277–284.

[4] Ettelaie C, Collier MEW, Featherby S, Greenman J, Maraveyas A. Peptidyl-prolyl isomerase 1 (Pin1) preserves the phosphorylation state of tissue factor and prolongs its release within microvesicles. Biochimica et Biophysica Acta. Molecular Cell Research. 2017; 1865: 12–24.

[5] Kurakula K, Koenis DS, Herzik MA, Liu Y, Craft JW, van Loenen PB, et al. Structural and cellular mechanisms of peptidyl-prolyl isomerase Pin1-mediated enhancement of Tissue Factor gene expression, protein half-life, and pro-coagulant activity. Haematologica. 2018; 103: 1073–1082.

[6] Lu KP, Hanes SD, Hunter T. A human peptidyl-prolyl isomerase essential for regulation of mitosis. Nature. 1996; 380: 544–547.

[7] Lu KP, Zhou XZ. The prolyl isomerase PIN1: a pivotal new twist in phosphorylation signalling and disease. Nature Reviews. Molecular Cell Biology. 2007; 8: 904–916.

[8] Liou Y, Zhou XZ, Lu KP. Prolyl isomerase Pin1 as a molecular switch to determine the fate of phosphoproteins. Trends in Biochemical Sciences. 2011; 36: 501–514.

[9] Zhou XZ, Kops O, Werner A, Lu PJ, Shen M, Stoller G, et al. Pin1-dependent prolyl isomerization regulates dephosphorylation of Cdc25C and tau proteins. Molecular Cell. 2000; 6: 873–883.

[10] Wulf G, Finn G, Suizu F, Lu KP. Phosphorylation-specific prolyl isomerization: is there an underlying theme? Nature Cell Biology. 2005; 7: 435–441.

[11] Siepe D, Jentsch S. Prolyl isomerase Pin1 acts as a switch to control the degree of substrate ubiquitylation. Nature Cell Biology. 2009; 11: 967–972.

[12] Jentsch S, Siepe D. Pin1, a novel switch in the ubiquitin pathway. Cell Cycle. 2009; 8: 3800–3801.

[13] Braithwaite AW, Del Sal G, Lu X. Some p53-binding proteins that can function as arbiters of life and death. Cell Death and Differentiation. 2006; 13: 984–993.

[14] Tong Y, Ying H, Liu R, Li L, Bergholz J, Xiao ZX. Pin1 inhibits PP2A-mediated Rb dephosphorylation in regulation of cell cycle and S-phase DNA damage. Cell Death Disease 2015; 6: e1640

[15] Shaw PE. Peptidyl-prolyl cis/trans isomerases and transcription: is there a twist in the tail? EMBO Reports. 2007; 8: 40–45.

[16] Kuang J, Ashorn CL, Gonzalez-Kuyvenhoven M, Penkala JE. Cdc25 is one of the MPM-2 antigens involved in the activation of maturation-promoting factor. Molecular Biology of the Cell. 1994; 5: 135–145.

[17] Ranganathan R, Lu KP, Hunter T, Noel JP. Structural and functional analysis of the mitotic rotamase Pin1 suggests substrate recognition is phosphorylation dependent. Cell. 1997; 89: 875–886.

[18] Lippens G, Landrieu I, Smet C. Molecular mechanisms of the phospho-dependent prolyl cis/trans isomerase Pin1. The FEBS Journal. 2007; 274: 5211–5222.

[19] Rajbhandari P, Schalper KA, Solodin NM, Ellison-Zelski SJ, Ping Lu K, Rimm DL, et al. Pin1 modulates ERα levels in breast cancer through inhibition of phosphorylation-dependent ubiquitination and degradation. Oncogene. 2014; 33: 1438–1447.

[20] Ettelaie C, Collier ME, Featherby S, Greenman J, Maraveyas A. Oligoubiquitination of tissue factor on Lys255 promotes Ser253-dephosphorylation, terminates TF release. Biochim Biophys Acta. 2016; 1863: 2846–2857.

[21] Rak J, Milsom C, Yu J. Tissue factor in cancer. Current Opinion in Hematology. 2008; 15: 522–528.

[22] Schaffner F, Ruf W. Tissue Factor and PAR2 Signaling in the Tumor Microenvironment. Arteriosclerosis, Thrombosis, and Vascular Biology. 2009; 29: 1999–2004.

[23] Åberg M, Siegbahn A. Tissue factor non-coagulant signaling - molecular mechanisms and biological consequences with a focus on cell migration and apoptosis. Journal of Thrombosis and Haemostasis. 2013; 11: 817–825.

[24] ElKeeb AM, Collier MEW, Maraveyas A, Ettelaie C. Accumulation of tissue factor in endothelial cells induces cell apoptosis, mediated through p38 and p53 activation. Thrombosis and Haemostasis. 2015; 114: 364–378.

[25] Alkistis Frentzou G, Collier MEW, Seymour AL, Ettelaie C. Differential induction of cellular proliferation, hypertrophy and apoptosis in H9c2 cardiomyocytes by exogenous tissue factor. Molecular and Cellular Biochemistry. 2010; 345: 119–130.

[26] Madkhali Y, Featherby S, Collier ME, Maraveyas A, Greenman J, Ettelaie C. The Ratio of Factor VIIa:Tissue Factor Content within Microvesicles Determines the Differential Influence on Endothelial Cells. THOpen. 2019; 3: e132–e145.

[27] Ethaeb AM, Mohammad MA, Madkhali Y, Featherby S, Maraveyas A, Greenman J, et al. Accumulation of tissue factor in endothelial cells promotes cellular apoptosis through overactivation of Src1 and involves β1-integrin signalling. Apoptosis. 2020; 25: 29–41.

[28] Pradier A, Ettelaie C. The influence of exogenous tissue factor on the regulators of proliferation and apoptosis in endothelial cells. Journal of Vascular Research. 2008; 45: 19–32.

[29] Mantovani F, Gostissa M, Collavin L, Del Sal G. KeePin' the p53 family in good shape. Cell Cycle. 2004; 3: 905–911.

[30] Haupt Y. P53 Regulation: a family affair. Cell Cycle. 2004; 3: 884–885.

[31] Zheng H, You H, Zhou XZ, Murray SA, Uchida T, Wulf G, et al. The prolyl isomerase Pin1 is a regulator of p53 in genotoxic response. Nature. 2002; 419: 849–853.

[32] Cohen M, Wuillemin C, Bischof P. Trophoblastic p53 is stabilised by a cis-trans isomerisation necessary for the formation of high molecular weight complexes involving the N-terminus of p53. Biochimie. 2008; 90: 855–862.

[33] Zhou XZ, Lu KP. The isomerase PIN1 controls numerous cancer-driving pathways and is a unique drug target. Nature Reviews. Cancer. 2016; 16: 463–478.

[34] Yu JH, Im CY, Min SH. Function of PIN1 in Cancer Development and Its Inhibitors as Cancer Therapeutics. Frontiers in Cell and Developmental Biology. 2020; 8: 120.

[35] Potter AJ, Ray S, Gueritz L, Nunns CL, Bryant CJ, Scrace SF, et al. Structure-guided design of alpha-amino acid-derived Pin1 inhibitors. Bioorganic & Medicinal Chemistry Letters. 2010; 20: 586–590.

[36] Potter A, Oldfield V, Nunns C, Fromont C, Ray S, Northfield CJ, et al. Discovery of cell-active phenyl-imidazole Pin1 inhibitors by structure-guided fragment evolution. Bioorganic & Medicinal Chemistry Letters. 2010; 20: 6483–6488.

[37] Ettelaie C, Collier MEW, Mei MP, Xiao YP, Maraveyas A. Enhanced binding of tissue factor-microparticles to collagen-IV and fibronectin leads to increased tissue factor activity in vitro. Thrombosis and Haemostasis. 2013; 109: 61–71.

[38] Bonnekoh B, Wevers A, Jugert F, Merk H, Mahrle G. Colorimetric growth assay for epidermal cell cultures by their crystal violet binding capacity. Archives of Dermatological Research. 1989; 281: 487–490.

[39] TiterTACS™. Colorimetric Apoptosis Detection Kit protocol. 2018. Available at: https://resources.rndsystems.com/pdfs/data sheets/4822-96-k.pdf (Accessed: 1 October 2021).

[40] Janowski B, Wöllner S, Schutkowski M, Fischer G. A protease-free assay for peptidyl prolyl cis/trans isomerases using standard peptide substrates. Analytical Biochemistry. 1997; 252: 299–307.

[41] Livak KJ, Schmittgen TD. Analysis of Relative Gene Expression Data Using Real-Time Quantitative PCR and the 2^{-CT} Method. Methods. 2001; 25: 402–408.

[42] Manders EMM, Stap J, Brakenhoff GJ, Vandriel R, Aten JA. Dynamics of 3-dimensional replication patterns during the S-phase, analyzed by double labeling of DNA and confocal microscopy. Journal of Cell Science. 1992; 103: 857–862.

[43] Manders EMM, Verbeek FJ, Aten JA. Measurement of colocalization of objects in dual-color confocal images. Microscopy. 1993; 169: 375–382.

[44] Morris GM, Huey R, Lindstrom W, Sanner MF, Belew RK, Goodsell DS, Olson AJ. AutoDock4 and AutoDockTools4: Automated docking with selective receptor flexibility. Journal of Computational Chemistry. 2009; 30: 2785–2791.

[45] Han H, Choi BY, Surh Y. Dual Roles of Pin1 in Cancer Development and Progression. Current Pharmaceutical Design. 2017; 23: 4422–4425.

[46] Nakatsu Y, Yamamotoya T, Ueda K, Ono H, Inoue M, Matsunaga Y, et al. Prolyl isomerase Pin1 in metabolic reprogramming of cancer cells. Cancer Letters. 2020; 470: 106–114.

[47] Matsuura I, Chiang K, Lai C, He D, Wang G, Ramkumar R, et al. Pin1 promotes transforming growth factor-beta-induced migration and invasion. The Journal of Biological Chemistry. 2010; 285: 1754–1764.

[48] Paneni F, Costantino S, Castello L, Battista R, Capretti G, Chiandotto S, et al. Targeting prolyl-isomerase Pin1 prevents mitochondrial oxidative stress and vascular dysfunction: insights in patients with diabetes. European Heart Journal. 2015; 36: 817–828.

[49] Jeong HG, Pokharel YR, Lim SC, Hwang YP, Han EH, Yoon J, et al. Novel Role of Pin1 Induction in Type II Collagen-Mediated Rheumatoid Arthritis. The Journal of Immunology. 2009; 183: 6689–6697.

[50] Zelaya H, Rothmeier AS, Ruf W. Tissue factor at the crossroad of coagulation and cell signaling. Journal of Thrombosis and Haemostasis. 2018; 16: 1941–1952.

[51] Rondon AMR, Kroone C, Kapteijn MY, Versteeg HH, Buijs JT. Role of Tissue Factor in Tumor Progression and Cancer-Associated Thrombosis. Seminars in Thrombosis and Hemostasis. 2019; 45: 396–412.

[52] Hisada Y, Mackman N. Tissue Factor and Cancer: Regulation, Tumor Growth, and Metastasis. Seminars in Thrombosis and Hemostasis. 2019; 45: 385–395.

[53] Featherby S, Madkhali Y, Maraveyas A, Ettelaie C. Apixaban Suppresses the Release of TF-Positive Microvesicles and Restrains Cancer Cell Proliferation through Directly Inhibiting TF-fVIIa Activity. Thrombosis and Haemostasis. 2019; 119: 1419–1432.

[54] Featherby S, Xiao YP, Ettelaie C, Nikitenko LL, Greenman J, Maraveyas A. Low molecular weight heparin and direct oral anticoagulants influence tumour formation, growth, invasion and vascularisation by separate mechanisms. Scientific Reports. 2019; 9: 6272.

[55] Pinch BJ, Doctor ZM, Nabet B, Browne CM, Seo H, Mohardt ML, et al. Identification of a potent and selective covalent Pin1 inhibitor. Nature Chemical Biology. 2020; 16: 979–987.

[56] Campaner E, Rustighi A, Zannini A, Cristiani A, Piazza S, Ciani Y, et al. A covalent PIN1 inhibitor selectively targets cancer cells by a dual mechanism of action. Nature Communications. 2017; 8: 15772.

[57] Lufei C, Cao X. Nuclear import of Pin1 is mediated by a novel sequence in the PPIase domain. FEBS Letters. 2009; 583: 271–276.

[58] Born A, Henen MA, Vögeli B. Activity and Affinity of Pin1 Variants. Molecules. 2019; 25: 36.

[59] Collier ME, Mei PM, Xiao YP, Maraveyas, A, Ettelaie C. The uptake of tumour cell-derived microparticles by microvascular endothelial cells results in the recycling of tissue factor to the cell surface with enhanced activity, in vitro. Thrombosis and Haemostasis. 2013; 110: 966–976.

Send correspondence to: Camille Ettelaie, Biomedical Section, University of Hull, Cottingham Road, HU6 7RX Hull, UK, E-mail: C.Ettelaie@hull.ac.uk